

# Iris Recognition: Preliminary Assessment about the Discriminating Capacity of Visible Wavelength Data

Gil Santos\*, Marco V. Bernardo\*, Hugo Proença\* and Paulo T. Fiadeiro†

\* Dept. of Informatics, Instituto de Telecomunicações - Networks and Multimedia Group

† Dept. of Physics, Remote Sensing Unit - Optics, Optometry and Vision Sciences Group

University of Beira Interior, Covilhã, Portugal

Email: gmelfe@ubi.pt, mbernardo@ubi.pt, hugomcp@di.ubi.pt, fiadeiro@ubi.pt

**Abstract**—The human iris supports contactless data acquisition and can be imaged covertly. These factors give raise to the possibility of performing biometric recognition procedure without subjects' knowledge and in uncontrolled data acquisition scenarios. The feasibility of this type of recognition has been receiving increasing attention, as is of particular interest in visual surveillance, computer forensics, threat assessment, and other security areas. In this paper we stress the role played by the spectrum of the visible light used in the acquisition process and assess the discriminating iris patterns that are likely to be acquired according to three factors: type of illuminant, its luminance, and levels of iris pigmentation. Our goal is to perceive and quantify the conditions that appear to enable the biometric recognition process with enough confidence.

**Keywords**-biometrics, iris recognition, visible light data, controlled standard illumination

## I. INTRODUCTION

Due to the effectiveness proven by the deployed iris recognition systems, the popularity of the iris as biometric trait has considerably grown over the last few years. A number of reasons justify this interest: it is a naturally protected internal organ visible from the exterior, it has a near circular and planar shape and its texture has a predominantly randotypic chaotic appearance. The typical scenarios where iris recognition systems were successfully deployed are quite constrained: subjects stop-and-stare relatively close to the acquisition device while their eyes are illuminated by a *near infrared* (NIR) light source that enables the acquisition of good quality data. Recently, several research initiatives have sought to increase capture distance and relax constraints on iris acquisition systems, making use of *visible wavelength* (VW) light imagery to covertly perform data acquisition (e.g. [1]), which broads the iris recognition applicability to forensic domains where the cooperation of the subjects is not expectable.

It is known that the VW light imagery engenders notorious differences in the appearance of the captured data when compared with the traditional NIR constrained setup (Figure 1). However, the acquisition of iris data from significantly larger distances and on moving targets demands simultaneously high f-numbers and very short exposure times for the optical system, in order to obtain acceptable depth-of-field



(a) NIR image, acquired under highly constrained conditions (WVU database [2]). (b) VW image, acquired under less constrained conditions (UBIRIS database [3]).

Figure 1. Comparison between the appearance of NIR and VW images.

values. These are in direct proportion with the amount of light required to proper imaging, which is a concern as excessively strong illumination can cause permanent eye damage. The American and European standards councils ([4] and [5]) proposed safe irradiance limits for NIR illumination of near  $10 \text{ mW/cm}^2$ . The NIR wavelength is particularly hazardous, because the eye does not instinctively respond with its natural mechanisms (aversion, blinking and pupil contraction).

The Eumelanin molecule is predominant in the human iris pigment [6] and has most of its radiative fluorescence under the VW light, which enables the capture of a much higher level of detail, but also of many more noisy artifacts: specular and diffuse reflections and shadows. Also, the spectral radiance of the iris in respect of the levels of its pigmentation varies much more significantly in the VW than in the NIR (Figure 2). These biological features usually engender acquired data with several other types of information within the iris rings: eyelashes, eyelids, specular and diffuse reflections obstruct portions of the iris texture and increase the challenges in performing accurate recognition.

The feasibility of the VW iris recognition remains controversial — specially for high pigmented irises that constitute the majority of the world's population — and fundamental research remains to be done. Hence, this paper gives — whenever possible — preliminary assessments about the

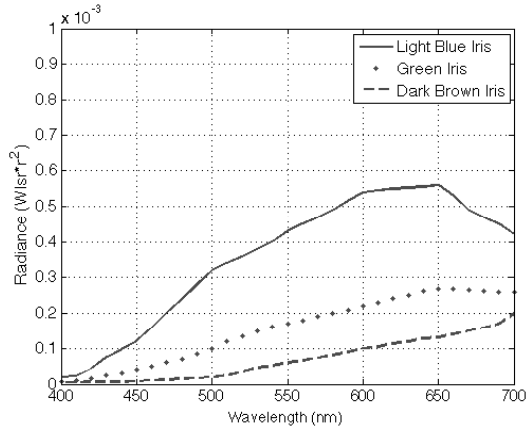


Figure 2. Spectral radiance of the human iris according to the levels of iris pigmentation [7].

amount of discriminating data able to be captured in such acquisition setup, regarding the spectrum and intensity of the used light and the levels of iris pigmentation. Also, we report the biological structures of the iris that are most likely to be used in discriminating between individuals in the VW acquisition scenario.

The remainder of this paper is organized as follows: Section II overviews mainstream iris recognition techniques and efforts towards the reduction of the involved constrains; Section III describes the image acquisition framework and setup used for the purposes of this paper; Section IV reports the performed experiments and discusses our results; Finally, Section V concludes and points further work.

## II. IRIS RECOGNITION

Deployed iris recognition systems are mainly based on Daugman’s pioneering approach [8], and have proven their effectiveness in relatively constrained scenarios where images are acquired in the NIR spectrum (700-900 nm). Regardless a few innovations [9], the process consists in the segmentation of the iris pupillary and limbic boundaries followed by the translation into a double dimensionless pseudo-polar coordinate system, that gives invariance to scale and translation. This normalized data is convolved with a set of Gabor filters at multiple frequencies and orientations and the corresponding output quantized to one of four quadrants, extracting two bits of phase information per convolution. The fractional Hamming distance is used to match iris signatures and several comparisons of shifted data are performed to achieve invariance to rotation.

The acquisition constraints for effective recognition have been motivating serious research efforts. The “Iris-on-the-move” project [10] should be emphasized: It is a major example of engineering an image acquisition system to make the recognition process less intrusive for subjects. The goal is to acquire NIR close-up iris images as a subject walks

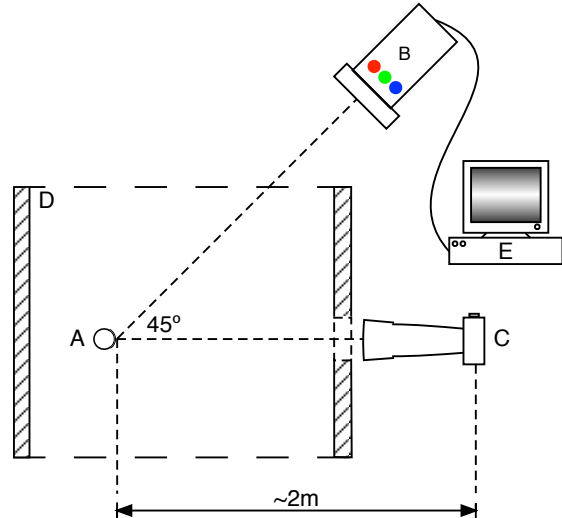


Figure 3. Acquisition setup. Subject (A) was positioned within an acquisition scene (D) and required to look forward, towards the camera (C) while illuminated at  $45^\circ$  by the RGB projector (B) controlled through a Visual Stimulus Generator (E).

at normal speed through an access control point. Previously, Fancourt et al. [11] concluded that it is possible to acquire sufficiently high-quality images at a distance of up to 10 meters. Smith et al. [12] examined the iris information that could be captured in the NIR and VW spectra, addressing the possibility of using these multispectral data to improve recognition performance.

## III. IMAGE ACQUISITION FRAMEWORK

The conceived acquisition setup was the one presented at Figure 3.

The subjects were placed in a dark acquisition scene, with their heads steady on a chin rest, and required to look forward towards the camera, which was placed at two meters and aligned with their right eyes. Varying the scene illuminant, produced by a *Barco RLM G5i Performer* (Barco Corporation, Belgian) RGB projector through a *Visual Stimulus Generator (VSG) 2/5* (Cambridge Research Systems, UK), images were captured by the Canon EOS 5D camera using the configuration in Table I.

Previously, the VSG generated stimulus were verified and calibrated using a telespectroradiometer (PR-650 *Spectra-Colorimeter*<sup>TM</sup>- Photo Research, Inc., CA) and a reference white  $BaSO_4$  sample placed on the chin rest. The maximum errors allowed were 0,002 illuminant chromaticities in the *Commission Internationale de l’Eclairage (CIE) 1931* ( $x, y$ ) space and  $1 \text{ cd/m}^2$  for luminance.

In order to mimic incandescent light, different phases of the daylight and fluorescent lamps, illuminants CIE A, D and F were picked as specified by the CIE 1931 standard colorimetric observer ( $2^\circ$ ) [13], [14]. Illuminants’ luminance was also controlled, regulated in uniform steps of  $20 \text{ cd/m}^2$ ,

Table I  
DETAILS OF IMAGE ACQUISITION SETUP.

Image Acquisition Framework and Setup	
Camera = Canon EOS 5D	Format = tiff
Color Representation = sRGB	F-Number = f/5.6
Shutter Speed = 1/8 sec	ISO Speed = ISO-400
Focal Length = 400 mm	Metering Mode = Spot
Width = 4368 pixels	Height = 2912 pixels
Resolution = 240 dpi	Bit Depth = 24 bit
Details of the Manually Cropped Resultant Images	
Width = 800 pixels	Height = 600 pixels
Format = tiff	Resolution = 240 dpi

Table II  
GENERATED ILLUMINANTS AND THEIR RESPECTIVE LUMINANCE.  
COMBINATIONS REPRESENTED BY × WERE NOT REPRODUCED AS THEY  
WERE OUT OF GAMUT ON THE RGB PROJECTOR.

		Luminance ( $cd/m^2$ )					
		20	40	60	80	100	120
Illuminant	A	✓	✓	✓	×	×	×
	D55	✓	✓	✓	✓	✓	×
	D65	✓	✓	✓	✓	✓	✓
	D75	✓	✓	✓	✓	✓	✓
	F11	✓	✓	✓	✓	×	×

from 20 to 120  $cd/m^2$ , producing the configurations shown in Table II.

According to this setup, 5 samples were consecutively acquired in each of the 24 scenarios (a specific illuminant at a certain luminance), delivering a total of 720 images. Such images came from 6 different subjects  $\{S_1, \dots, S_6\}$ , equally divided into light, medium and heavily pigmented irises.

#### IV. EXPERIMENTS

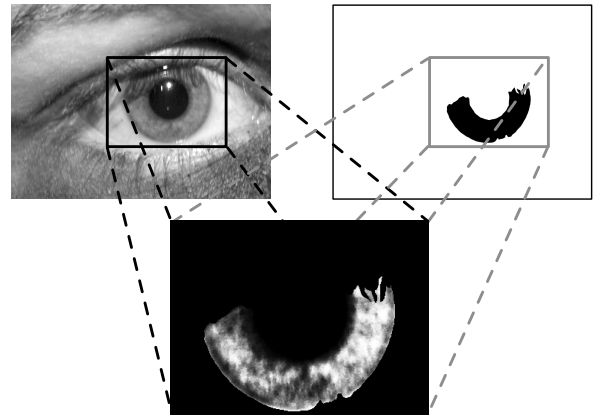
All irises were manually segmented (Figure 4a), avoiding that eventual errors were carried on to further experimental stages.

Both the pupillary and limbic iris boundaries were modeled as circles, and data was translated into a pseudo-polar dimensionless coordinate system (Figure 4b) in order to obtain invariance to scale and translation.

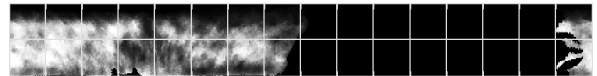
##### A. Visual Inspection

When comparing to the currently deployed iris recognition systems, there is a complexity gain in the VW image acquisition, as data become represented along three axis (usually Red, Green and Blue — RGB) instead of a single one.

However, our earliest analysis did not make use of this higher amount of information. Aiming at study the lumi-



(a) Merging of original image with manual segmentation.



(b) Normalized iris on pseudo-polar coordinates.

Figure 4. Illustration of the steps taken prior to visual inspection and color analysis.

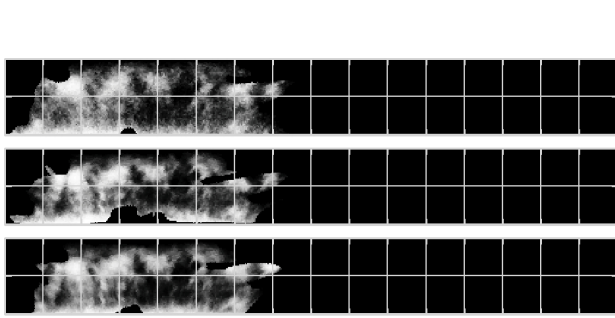
nance bounds that — under visual inspection — enable the capturing of discriminating patterns in the iris data, we found appropriate to reduce data dimensionality to the luminance channel (Y) of the YCbCr colorspace [15]. Later, we performed an equalization of each image histogram, so that the iris structure could be better distinguished.

We concluded that the easiness of detecting discriminating iris patterns varies proportionally to the illuminants' luminance level used in the acquisition, and is almost invariant to the type of used illuminant. For light pigmented irises, all the luminance levels on trial appeared to be propitious (Figure 5a). Oppositely, for highly pigmented ones, the detection of discriminating patterns has revealed as a much more difficult task, even using 120  $cd/m^2$  (Figure 5c). Medium pigmented irises have intermediate behavior, and luminance values higher than 60  $cd/m^2$  propitiate the capturing of discriminating iris patterns (Figure 5b). According to these observations, we found appropriate to define relatively large bounds for the amounts of light that enable the capturing of discriminating iris patterns, as given in Figure 6.

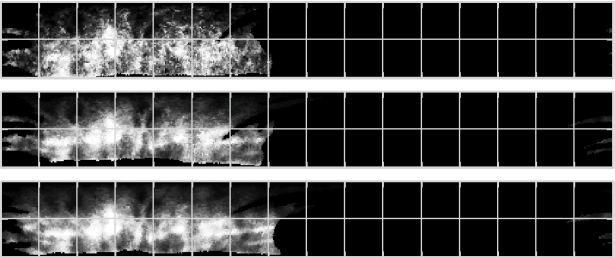
Also, it should be taken into account that the quantity of discriminating patterns able to be perceived under visual inspection is highly varying between different irises, although crypts and freckles were observed to be the most likely used to discriminate between individuals. For such, these bounds are regarded as rough initial values, that should be finely adjusted by further analysis.

Table III  
 CIELAB  $\bar{\Delta}E_{ab}^*$  ON POINT-TO-POINT IMAGE COMPARISONS, IN DIFFERENT ILLUMINANTS FOR BOTH INTRA- (I) AND INTER- (II) CLASSES, AT  $60 \text{ cd/m}^2$ . VALUES ARE PRESENTED FOR AN 95% CONFIDENCE INTERVAL.

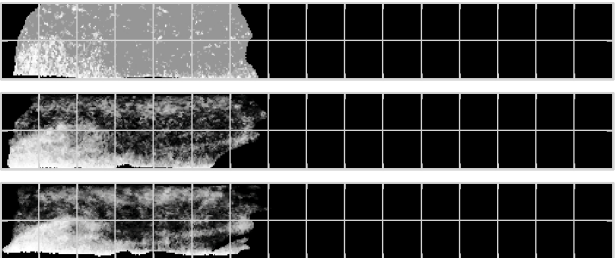
Illum.	Class	Heavy Pigmentation		Light Pigmentation		Medium Pigmentation	
		Subject 1	Subject 2	Subject 3	Subject 4	Subject 5	Subject 6
A	I	14,08 ± 4,01	14,15 ± 4,91	18,28 ± 4,57	17,71 ± 4,57	14,26 ± 4,20	14,19 ± 4,08
	II	22,06 ± 10,32	27,29 ± 11,17	19,11 ± 8,27	18,84 ± 8,15	23,46 ± 10,23	24,68 ± 9,95
D55	I	7,44 ± 4,91	8,03 ± 5,71	8,86 ± 7,84	9,08 ± 7,59	7,62 ± 6,15	8,22 ± 6,13
	II	17,51 ± 7,62	24,13 ± 9,35	27,87 ± 10,00	23,78 ± 9,79	15,42 ± 7,29	16,24 ± 7,37
D65	I	7,59 ± 5,79	8,10 ± 6,00	8,64 ± 7,90	8,55 ± 6,84	7,16 ± 5,93	7,16 ± 5,70
	II	17,74 ± 7,22	24,28 ± 8,89	28,21 ± 10,05	22,36 ± 9,28	15,49 ± 7,42	16,50 ± 7,57
D75	I	8,71 ± 6,27	8,83 ± 6,37	8,44 ± 7,61	8,72 ± 7,27	7,14 ± 5,82	7,25 ± 5,70
	II	17,84 ± 6,94	24,10 ± 8,66	27,77 ± 10,03	23,55 ± 9,76	15,53 ± 7,39	16,49 ± 7,54
F11	I	8,62 ± 2,64	8,46 ± 4,94	10,61 ± 1,09	10,12 ± 1,47	8,57 ± 1,72	8,43 ± 1,82
	II	18,77 ± 8,71	25,59 ± 10,23	21,98 ± 8,75	19,22 ± 7,87	18,27 ± 8,89	19,18 ± 8,76



(a) Light pigmented irises.



(b) Medium pigmented irises.



(c) Heavy pigmented irises.

Figure 5. Y channel histogram-equalized samples for different pigmentation levels, under CIE D65 illuminant, with 20, 60 and 120  $\text{cd/m}^2$  (top to bottom).

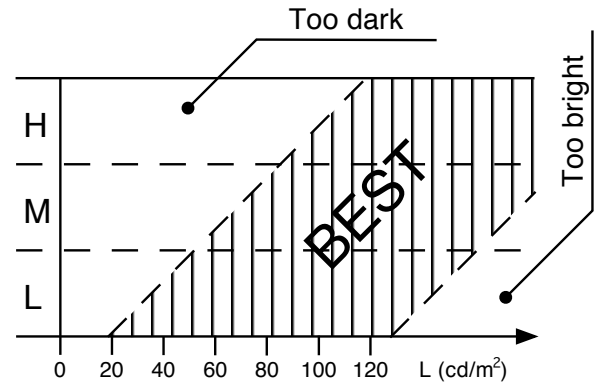


Figure 6. Best perceived luminance levels for high (H), medium (M) and low (L) pigmented irises.

### B. Color Analysis

Normalized images were converted to the CIE 1976 ( $L^*a^*b^*$ ) colorspace, also known as CIELAB, which is device independent, partially uniform and based on the human visual system, allowing absolute color representation according to the illuminant. We obtained the chromatic adaptation matrices using projector's CIE 1931 ( $x, y, Y$ ) phosphor coordinates and RGB coordinates of the reference white for each illuminant. We selected the images captured at an intermediate luminance level ( $60 \text{ cd/m}^2$ ), and performed a pixel-to-pixel color difference (chromatic error) between image pairs  $I_1$  and  $I_2$  as Equation 1.

$$\Delta E_{ab}^* = \sqrt{(L_1^* - L_2^*)^2 + (a_1^* - a_2^*)^2 + (b_1^* - b_2^*)^2} \quad (1)$$

Results were grouped into two distributions: intra-class for comparisons between the same eye and inter-class for different eyes, both captured in different illuminants. Inspecting those results, we observed that they fit the normal distributions detailed at Table III, also described through the Receiver Operator Characteristic (ROC) curves of Figure 7 and Table IV.

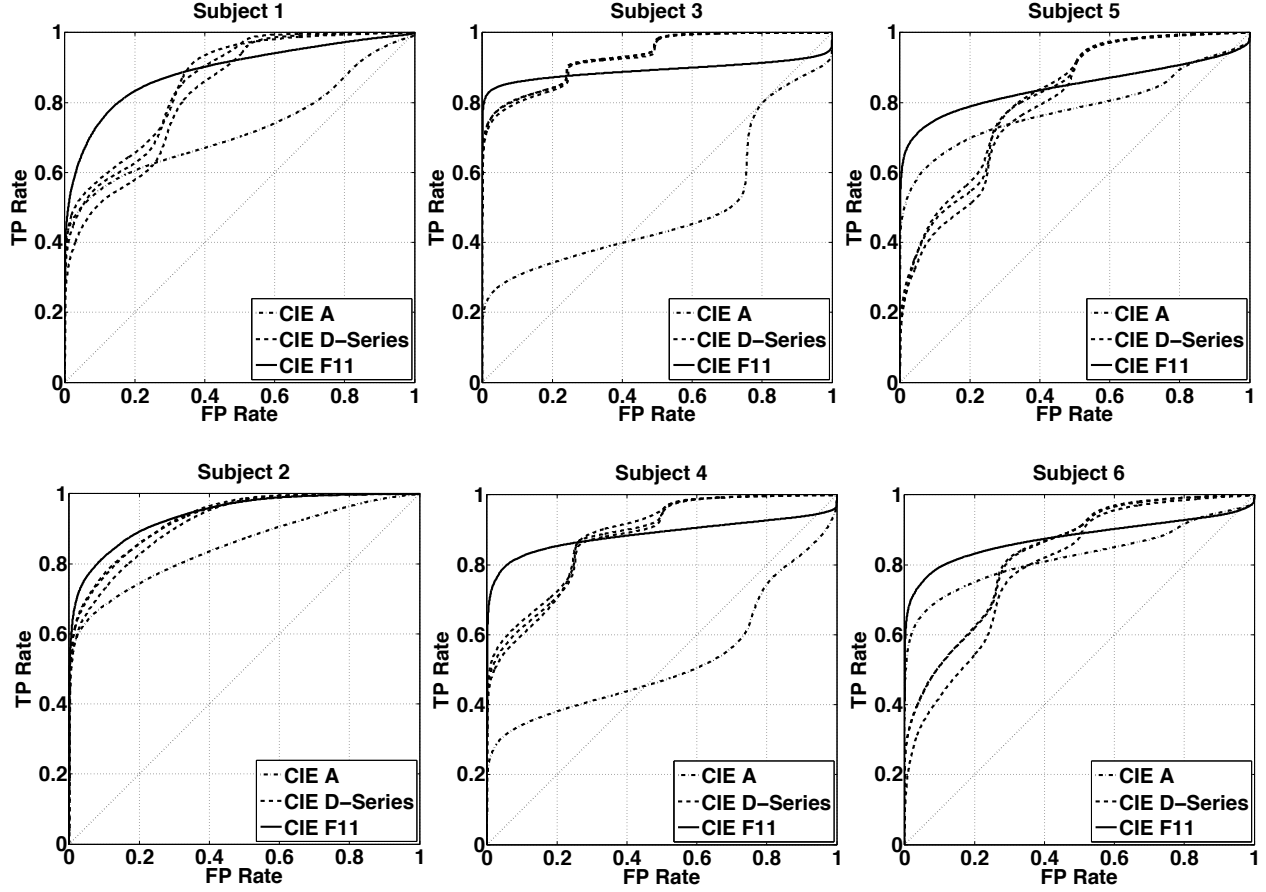


Figure 7. ROC Curves for all subjects, on different illuminants, at  $60 \text{ cd/m}^2$ .

Table IV  
AREA UNDER ROC CURVE FOR ALL SUBJECTS ON DIFFERENT ILLUMINANTS, AT  $60 \text{ cd/m}^2$ .

	S 1	S 2	S 3	S 4	S 5	S 6
A	0,724	0,850	0,501	0,527	0,781	0,824
D55	0,862	0,926	0,930	0,877	0,791	0,795
D65	0,855	0,930	0,934	0,880	0,808	0,834
D75	0,827	0,916	0,934	0,884	0,813	0,832
F11	0,890	0,940	0,892	0,886	0,845	0,876

It can be seen that results obtained for the CIE D55, D65 and D75 illuminants were very similar. The poorest matches occurred when data captured with a CIE D is compared to data captured with a CIE A illuminant. The CIE F11 illuminant, with a *Correlated Color Temperature* (CCT) between the ones of CIE D-Series and CIE A, is the one with better overall performance.

The upper image of Figure 8 illustrates the pixel usage in the obtainment of the pixel-to-pixel color distances.

Here, the darkest region at the left part of the normalized image (which corresponds to the lower part of the cartesian data), is the one more frequently considered as noise-free. The brightest part by other side, commonly occluded, was

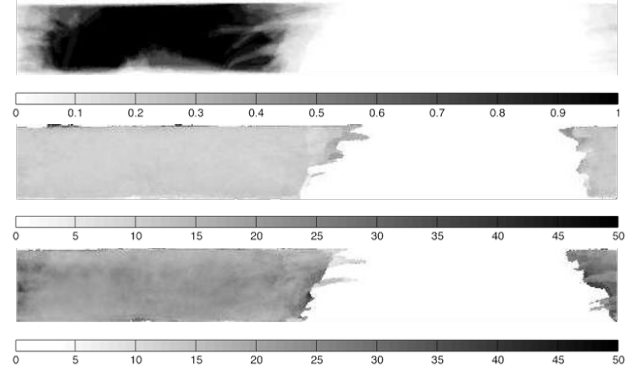


Figure 8. Pixel usage probability (top) and  $\bar{\Delta E}_{ab}^*$  values per pixel for intra (middle) and inter (bottom) classes.

rarely used for comparison purposes. The middle and bottom images give the  $\Delta E_{ab}^*$  average values ( $\bar{\Delta E}_{ab}^*$ ), enabling us to perceive the relative contribution of each iris region to the intra-class (middle image) and inter-class (bottom image) distance values. Relatively homogeneous values were obtained in both cases, with exception to the pupillary region, where the average chromatic error values  $\bar{\Delta E}_{ab}^*$  of

the inter-class comparisons tend to vanish close to the intra-class values. The obtained  $\bar{\Delta}E_{ab}^*$  values were  $9,82 \pm 6,36$  for the intra-class and  $21,21 \pm 9,77$  for the inter-class comparisons, with a 95% confidence interval. Thus, even an extremely simple image matching technique is able to produce a clear separability between the two classical types of comparisons.

## V. CONCLUSIONS AND FURTHER WORK

Although preliminary, performed experiments allowed us to conclude that the appearance of the captured iris pattern is poorly conditioned by the type of VW illuminant used in the acquisition, in opposition to the levels of luminance, that play a much more significant role.

The obtained pixel-to-pixel  $\Delta E_{ab}^*$  values appear to confirm that color information contained in VW data can be used to discriminate between different irises. Also, the CIE F11 illuminant should be preferably used in data enrollment, as it was the one that propitiated more compatibility between iris patterns acquired with all the remaining illuminants.

As further work, we plan to increase the statistical relevance of the described experiments — with both the inclusion of more test subjects and a subsequent higher range of pigmentation levels — and make use of more types of illuminants, so that CCT differences between them become more uniform and a larger area in the Planckian locus will be covered.

## ACKNOWLEDGMENT

The authors are very grateful for the support given by the Optical Center of the University of Beira Interior, and also for the financial support given by "FCT-Fundação para a Ciência e Tecnologia" and "FEDER" in the scope of the PTDC/EIA/69106/2006 ("BIOREC: Non-Cooperative Biometric Recognition") and PTDC/EIA-EIA/103945/2008 ("NECOVID: Covert Negative Biometric Identification") research projects.

## REFERENCES

- [1] C. Boyce, A. Ross, M. Monaco, L. Hornak and Xin Li. Multispectral Iris Analysis: A Preliminary Study. *Proceedings of Computer Vision and Pattern Recognition Workshop on Biometrics (CVPRW)*, New York, USA, June 2006.
- [2] A. Ross, S. Crihalmeanu, L. Hornak, and S. Schuckers. A centralized web-enabled multimodal biometric database. In *Proceedings of the 2004 Biometric Consortium Conference (BCC)*, U.S.A, September 2004.
- [3] H. Proença, S. Filipe, R. Santos, J. Oliveira and L. A. Alexandre. The UBIRIS.v2: A Database of Visible Wavelength Iris Images Captured On-The-Move and At-A-Distance. *IEEE Transactions on Pattern Analysis and Machine Intelligence*, vol. 99, 2009.
- [4] American National Standards Institute. American national standards for the safe use of lasers and LEDs used in optical fiber transmission systems, 1988. ANSI Z136.2.
- [5] Commission International de l'Eclairage. Photobiological safety standards for lamps, 1999. Report of TC 6-38; CIE 134-3-99.
- [6] P. Meredith and T. Sarna. The physical and chemical properties of eumelanin. *Pigment Cell Research*, vol. 19, pp. 572-594, 2006.
- [7] F. Imai. Preliminary experiment for spectral reflectance estimation of human iris using a digital camera. Technical report, Munsell Color Science Laboratories, Rochester Institute of Technology, 2000.
- [8] J. Daugman. How Iris Recognition Works. *IEEE Trans. CSVT* 14(1), pp. 21-30, 1993.
- [9] J. Daugman. New methods in iris recognition. *IEEE Trans. Systems, Man, Cybernetics B* 37(5), pp. 1167-1175, 2007.
- [10] J.R. Matey, D. Ackerman, J. Bergen, and M. Tinker. Iris Recognition in Less Constrained Environments. *Advances in Biometrics: Sensors, Algorithms and Systems*, pp. 107-131, Springer, Oct. 2007.
- [11] C. Fancourt, L. Bogoni, K. Hanna, Y. Guo, R. Wildes, N. Takahashi, and U. Jain. Iris Recognition at a Distance. *Proc. 2005 IAPR Conf. Audio and Video Based Biometric Person Authentication*, pp. 1-13, July 2005.
- [12] K. Smith, V.P. Pauca, A. Ross, T. Torgersen, and M. King. Extended Evaluation of Simulated Wavefront Coding Technology in Iris Recognition. *Proc. First IEEE Int'l Conf. Biometrics: Theory, Applications, and Systems*, pp. 1-7, Sept. 2007.
- [13] CIE Colorimetry. *CIE Publication 15:2004*, (CIE, Vienna, 2004).
- [14] T. Smith and J. Guild. The C.I.E. colorimetric standards and their use. *Transactions of the Optical Society* 33 (3): pp. 73-134, 1931-32.
- [15] A. Poynton. A technical introduction to digital video. John Wiley & Sons, Inc, New York, USA, 2006.